ISSN 1990-7931, Russian Journal of Physical Chemistry B, 2020, Vol. 14, No. 7, pp. 1–8. © Pleiades Publishing, Ltd., 2020.
Russian Text © The Author(s), 2020, published in Sverkhkriticheskie Flyuidy. Teoriya i Praktika, 2020, Vol. 15, No. 1, pp. 103–111.

Solvation of Ethanol, Phenol, and *o*-Methoxyphenol in Dilute Aqueous Solutions under Normal and Supercritical Conditions

E. S. Alekseev[a] and T. V. Bogdan[a, *]

[a] *Faculty of Chemistry, Moscow State University, Moscow, 119991 Russia*

**e-mail: chemist2014@yandex.ru*

Received November 19, 2019; revised December 4, 2019; accepted December 4, 2019

Abstract—The structure of 2 wt % aqueous solutions of ethanol, phenol, and *o*-methoxyphenol (guaiacol) was modeled in NVT ensemble using the classical molecular dynamics method at densities of 0.997 and 0.133 g/cm^3 corresponding to the normal (298 K, 0.1 MPa) and supercritical (673 K, 23.0 MPa) conditions. The self-diffusion coefficients were calculated for individual components in solutions; the radial distribution functions were calculated for the oxygen atoms of water molecules, oxygen atoms of hydroxyl groups, and centers of mass in phenol molecules. The possibility of clusterization of solute molecules was analyzed. The data obtained suggest heterogeneity of solutions, in which clusters of different compositions and structures can exist. Clusterization of up to seven ethanol and phenol molecules can occur under normal conditions, and dimerization was detected under SC conditions. The structural features of solutions under normal and SC conditions were compared. The difference in the formation of hydration shells of ethanol and phenol molecules was demonstrated. Stable shells of water molecules form around ethanol molecules under normal conditions. For phenols, the solvation shells are unstable, with a pronounced tendency toward clusterization of organic molecules.

Keywords: molecular dynamics, modeling, solvation, dilute aqueous solutions, normal conditions, supercritical conditions, water–ethanol, water–guaiacol, and water–phenol solutions, lignin, self-diffusion coefficient, clusterization

DOI: 10.1134/S1990793120070209

INTRODUCTION

Lignin is an irregular natural polymer whose monomer units contain a phenol fragment with hydroxyl, methoxy, and propyl groups. These units are connected with one another by bonds of various types, forming heterocyclic fragments. Lignin-containing materials are the most widespread natural recyclable resources, the vegetable world annually producing 170 million tons of lignin–containing raw materials [1]. Due to the availability and abundance of functional groups, lignin can serve as a raw material for the production of various chemical substances: phenols, alcohols, esters, acids, hydrocarbons, and new composite materials. Its high chemical stability, however, hinders its full employment, with only 2% of all industrial lignin currently used for production purposes [2].

Depolymerization of lignin in supercritical water (SCW) is one of the promising methods for its processing. However, studies of the chemical transformation of lignin are hindered by the irregular structure of the natural polymer and the strong dependence of the composition of reaction products on the type of the raw material used [3]. As direct structural studies are problematic under supercritical (SC) conditions, computer simulation is currently actively used. This makes it possible to see the structural and dynamic peculiarities of the reaction medium at the molecular level.

To correlate the reaction route with the composition of the lignin-containing raw material, it seems reasonable to initially study in detail the behavior of aqueous solutions of small molecules containing the functional fragments of natural lignin under normal and SC conditions. As the monomer units of lignin contain hydroxyl groups bonded with both the aromatic ring and the aliphatic fragments, here we studied the aqueous solutions of the model fragments of lignin: ethanol (**1**), phenol (**2**), and *o*-methoxyphenol (guaiacol) (**3**) under normal and SC conditions:

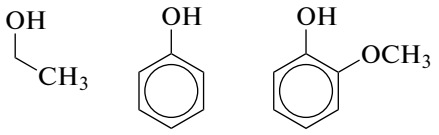

1 **2** **3**

The ethanol and phenol molecules serve as models for studying the interactions of the aliphatic groups and aromatic fragments of lignin with water molecules, respectively, and the behavior of guaiacol mole-

Table 1. Parameters of computation schemes (all concentrations correspond to 2 wt %)

Parameter	System					
	ethanol–water		phenol–water		guaiacol–water	
Mole fraction of alcohol or phenol	0.008		0.004		0.003	
Number of molecules in the computation cell: water/alcohol (phenol)/total	9920/80/10000		9960/40/10000		9970/30/10000	
Temperature, K	298	673	298	673	298	673
Pressure, MPa	0.1	23.0	0.1	23.0	0.1	23.0
Cell edge, nm	6.72	3.13	6.77	13.15	6.73	13.16

cules shows the role of substituents in the benzene ring in solvation of the aromatic molecule. Here, as in the experimental studies of the routes of chemical transformations of similar compounds in SCW [4, 5], the alcohol and phenol concentration was chosen to be 2 wt %.

In recent years, the compounds chosen here have remained a subject of unfailing interest from both theoretical and practical viewpoints because of studies of reactions of organic compounds with water under SC conditions [6], especially those that form gaseous products, and also in view of the use of ethanol and phenol as co-solvents in reactions of organic substances in SCW [3]. We focused on comparison of the dynamic and structural characteristics of solutions of compounds **1**–**3** on passing from normal to SC conditions.

CALCULATION PROCEDURE

The classical molecular dynamic simulation of the structure of aqueous solutions containing 2 wt % organic component (ethanol, phenol, and guaiacol) in NVT ensemble at densities of 0.997 g/cm^3 and 0.133 g/cm^3 corresponding to the normal (298 K, 0.1 MPa) and supercritical (673 K, 23.0 MPa) conditions. The modeling used GROMACS program package [7], OPS-AA potential [8] for ethanol and phenols, and the TIP4P model [9] for water. The nonvalent interactions were described in the form of pair terms including the 6–12 (Lennard-Jones) potential and the Coulomb potential. The cross terms were described using the modified Lorentz–Berthelot rule, which defines the parameters of the Lennard-Jones potential (σ and ε) between various force centers (i, j) as a mean arithmetic:

$$\sigma_{ij} = (\sigma_{ii}\sigma_{jj})^{1/2}; \quad \varepsilon_{ij} = (\varepsilon_{ii}\varepsilon_{jj})^{1/2}.$$

The total number of molecules in the computation cell was 10000. At the same mass fraction of ethanol and phenols in solutions, their mole concentrations differed (Table 1).

At first, low-density cells with random location of solute molecules were constructed; then water molecules were added to the cell. At the next stage, the cell density was set to the given value by changing the volume of the cubic cell. In view of the low solute concentration, we used the densities for water: 0.997 g/cm^3 for 298 K and 0.1 MPa and 0.133 g/cm^3 (the calculated value) for 673 K and 23.0 MPa [10]. The energy of the model systems was minimized by the steepest descent method with an initial step of 0.01 nm using the GROMACS program package. The energy minimization was performed as long as the force that acted on one atom exceeded 10 kJ/(mol nm). For integrating the equations of motion, we used the leap-frog algorithm with an integration step of 0.001 ps. The temperature was maintained at a constant level using a Nosé–Hoover thermostat. The Coulomb interactions were calculated using particle-mesh Ewald's (PME) algorithm with a trimming radius of 10 Å. The trimming radius of van der Waals interactions was also 10 Å. The system was thermostatted for 10 ns; then molecular dynamic trajectories were recorded for 10 ns for analysis while recording the coordinates and rates every 0.5 ps. The trajectories were analyzed using the GROMACS program package [7].

The radial distribution functions (RDFs) of the interatomic distances were calculated by the equation

$$g(r) = \frac{\left\langle \sum_{i,j} \delta(r - r_{ij}) \right\rangle}{4\pi\rho r^2} \Delta r,$$

where r_{ij} is the distance between the atoms, and ρ is the number density of molecules at distances in the range of Δr.

Thus, the RDFs of distances between oxygen atoms were constructed for water, between the hydroxyl oxygen atoms for compounds **1**–**3** (which provides data on hydrogen bonds), and also between the centers of benzene rings for phenols **2** and **3**.

The self-diffusion coefficients D for individual substances were determined from the mean-square displacements of the centers of mass of molecules using the approximation

$$D = \lim \frac{1}{6Nt} \left\langle \sum_N [r_i(t) - r_i(0)]^2 \right\rangle,$$

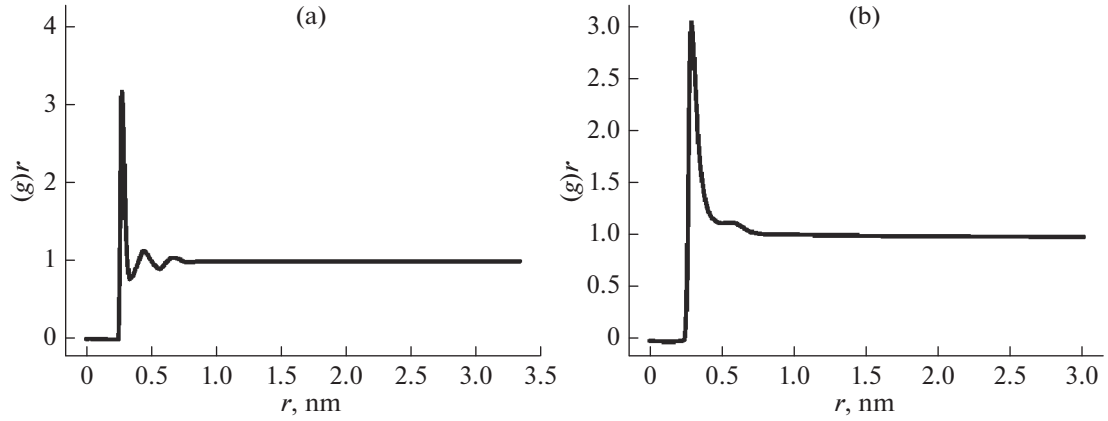

Fig. 1. Radial distribution functions for the oxygen–oxygen distances of water molecules under (a) normal and (b) supercritical conditions.

where $r_i(t)$ are the coordinates of the center of mass of the molecule at a moment of time t; and N is the number of molecules.

The self-diffusion coefficients averaged over solution were calculated as the mean arithmetic for particles of all types taking into account their mole fraction in solution:

$$D_{av} = (D_w N_w + D_s N_s)/(N_w + N_s),$$

where D_w and D_s are the self-diffusion coefficients of water and solute, respectively; N_w and N_s are the numbers of water and solute molecules, respectively, in the system.

The clusterization of solute molecules was studied using the program for cluster isolation implemented in the GROMACS package. The program allows unification of molecules in a cluster if the distance between two arbitrary atoms of two molecules is smaller than the given trimming radius. In this way we obtained data on the number of clusters and their size during the simulation. For cluster isolation we used the distance between non-hydrogen atoms as a geometrical criterion, which equals 0.35 nm; it defines the interatomic interaction, on the one hand, and limits the possible cluster configurations to direct contacts of molecules.

RESULTS AND DISCUSSION

Figure 1 shows the RDFs for oxygen–oxygen distances in water under normal and supercritical conditions. The state of water in the systems depends only on the external conditions (temperature and pressure) and is independent of the nature of the solute. The RDFs have three maxima under normal conditions, which reflect tetrahedral ordering in the structure of water. Under the supercritical conditions (23.0 MPa, 673 K), the first maximum is considerably broadened compared to that under normal conditions, the minimum between the first and second maxima is absent, the second maximum vanished except the shoulder adjacent to the first maximum, and the third peak diffused. This form of RDFs for SC conditions shows the presence of inhomogeneities in the instant structure of the water fluid in the given region of the phase diagram. The authors of several experimental works observed inhomogeneities of this kind and regarded them as evidence for the existence of liquid-like and gas-like regions in the fluid [11]. However, there are quite different approaches to the interpretation of experimental data on the RDFs for water in the SC state (see, e.g., [12]).

Figure 2 shows the RDFs of O–O for the hydroxyl group of molecules **1**–**3** at different steps of modeling. The RDF maxima in the region of 0.3 nm reflect the hydrogen bonding between ethanol and phenol molecules. The absence of maxima at 0.3 nm at the individual steps of the trajectory indicates that the hydrogen bonds between the solute molecules are unstable.

Under normal conditions, the time-averaged RDF for the O–O distances of hydroxyl groups (colored insert, Fig. 2) has a wide maximum in the region 0.3–0.7 nm, which corresponds to the existence of clusters in which the solute molecules are hydrogen-bonded both directly with one another and via the oxygen atoms of the water molecules. Under the SC conditions, the first maximum also appears at a distance of 0.35 nm at definite steps of the trajectory; this suggests that short-lived hydrogen bonds appeared between the hydroxyl groups of organic molecules, i.e., that the system contains solute molecules not solvated by water molecules but interacting with one another.

The averaged RDF for the O–O distances of hydroxyl groups has no maximum under SC conditions, indicating that the hydrogen bonds are unstable at increased temperature and pressure. Guaiacol showed more pronounced tendency toward agglomeration of molecules through hydrogen bonding at some

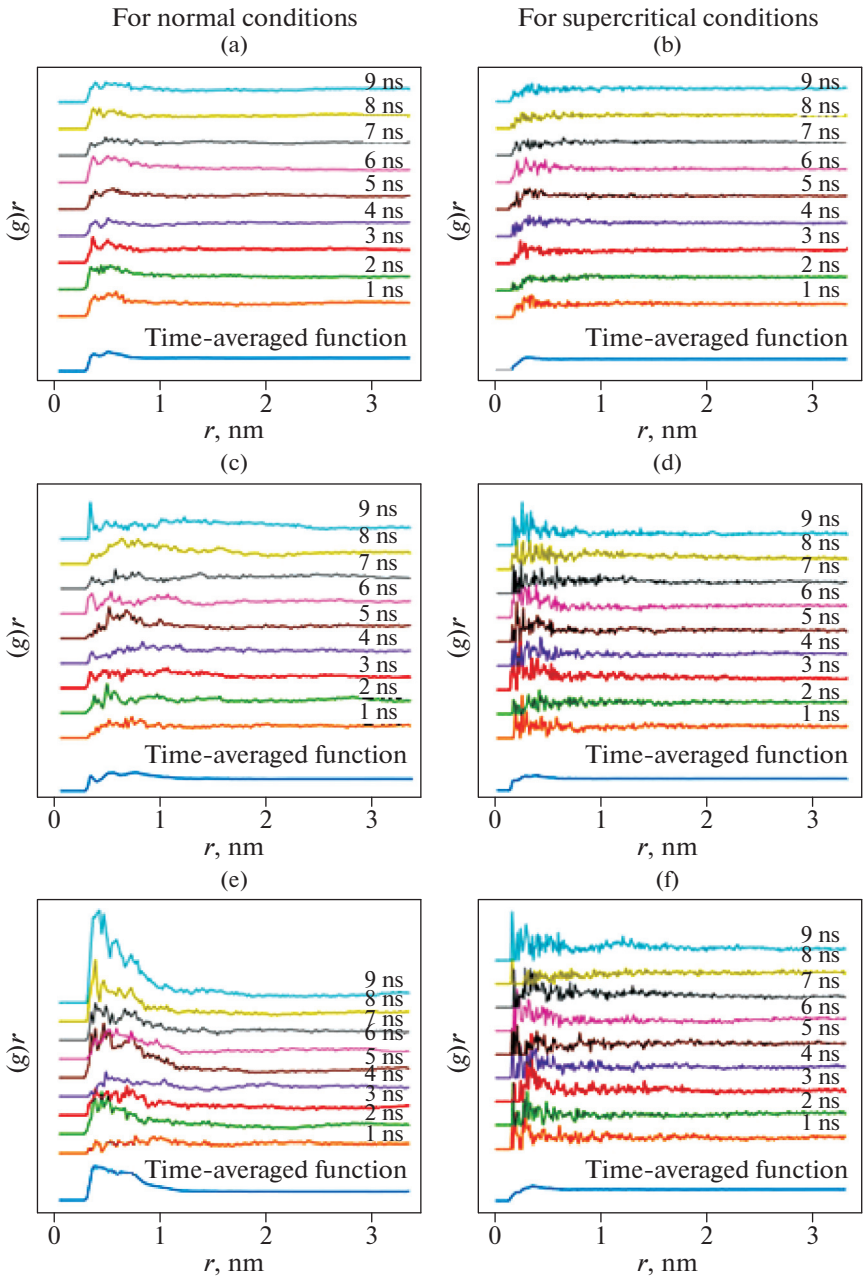

Fig. 2. Radial distribution functions for the distances of oxygen atoms of (a, b) ethanol; (c, d) phenol; and (e, f) guaiacol molecules at different steps of modeling for (a, c, e) normal and (b, d, f) supercritical conditions. The curves for different trajectory steps are shifted relative to one another by 1.

trajectory steps than for ethanol and phenol for both normal and SC conditions.

As clusterization of molecules **2**–**3** is also possible due the specific contacts of benzene rings [13], we calculated the RDFs for the centers of mass of these molecules (colored insert, Fig. 3). The wide maximum at 0.5–0.7 nm on the averaged function for normal conditions (Fig. 3a) corresponds to clusterization of molecules with different mutual orientations. The shift of the maximum to 0.5 nm indicates that the phenol molecules lie in the first coordination sphere of one another. The data of Figs. 3b and 3d show the dynamics of clusterization: the maximum at 0.5 nm vanishes and again appears with time. On passing to SC conditions, the first maximum is broadened to 1 nm, but the peak at 0.5 nm exists at some trajectory steps, indicating the presence of short-lived clusters.

Figures **1**–**3** show the data for the individual steps of the trajectories. Table 2 lists the calculated self-diffusion coefficients (D) for each component of solution

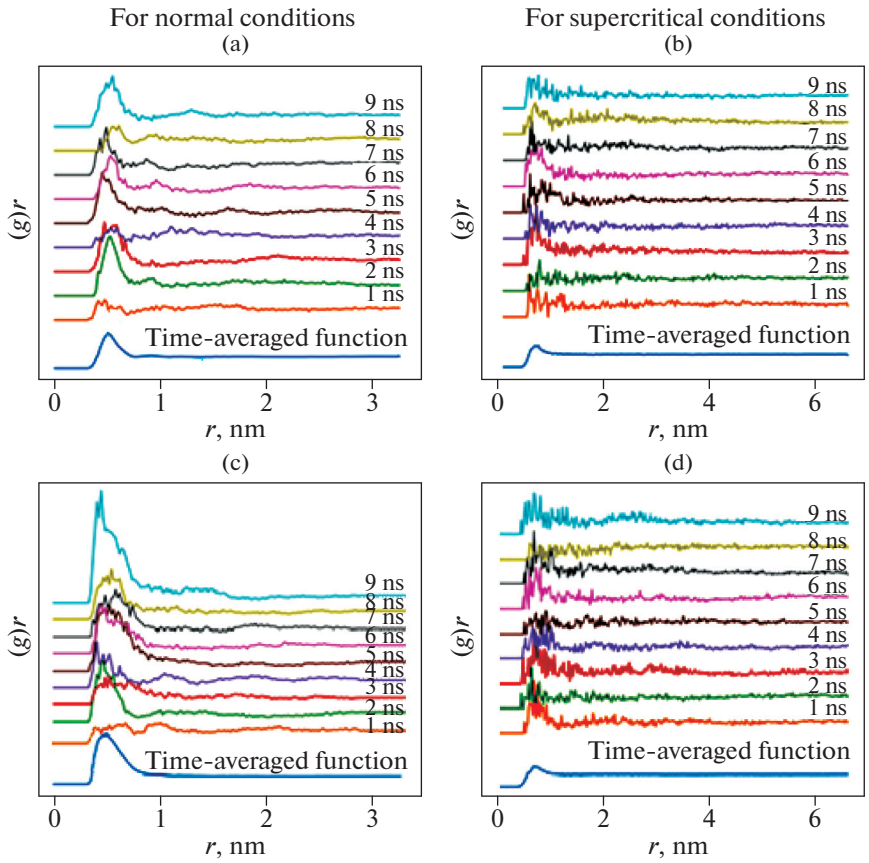

Fig. 3. Radial distribution functions for the centers of mass of (a, b) phenol and (c, d) guaiacol molecules for (a, c) normal and (b, d) supercritical conditions at different trajectory steps and time-averaged function.

and the values averaged over solution, which coincide almost completely for all systems under the same conditions as the main contribution to D_{av} is from water molecules at low solute concentrations. Under normal conditions, D for ethanol is higher than for phenol and guaiacol by a factor of 1.5 to 2. On passing from normal to SC conditions, D increases for all molecules: 55-fold for water, 60-fold for ethanol, and 40–50-fold for phenol and guaiacol. While for phenol and guaiacol D is three times smaller than for water, for ethanol the difference is only 1.4-fold (under SC conditions). Thus, in the SC region, the ethanol molecules move at rates closest to those of the motion of water molecules.

The relative deviation of D for solute molecules from the average values is much more significant than

Table 2. Self-diffusion coefficients for solute and water molecules and average values over solution

Self-diffusion coefficient	Solute component		
	ethanol	phenol	guaiacol
$\rho = 0.997$ g/cm^3 (298 K; 0.1 MPa)			
Solute	1.87 ± 0.23	1.26 ± 0.18	0.97 ± 0.12
Water	2.91 ± 0.03	2.96 ± 0.03	2.95 ± 0.01
Average over solution	2.88 ± 0.03	2.93 ± 0.02	2.91 ± 0.01
$\rho = 0.133$ g/cm^3 (673 K; 23.0 MPa)			
Solute	113.00 ± 22.00	51.00 ± 14.00	50.00 ± 2.00
Water	162.00 ± 1.00	162.00 ± 2.00	163.00 ± 4.00
Average over solution	161.00 ± 1.00	160.00 ± 2.00	161.00 ± 4.00

for water molecules. This can be explained by the inhomogeneity of the structure of solutions and supercritical fluids: for example, by the formation of clusters consisting of solute molecules and aqueous-organic clusters. The self-diffusion coefficient of ethanol is closest to the values for water, which is explained by the relative closeness of the size and mass of water molecules to the same characteristics of ethanol (compared with those of phenol), the inclusion of ethanol molecules in the water clusters under both normal and SC conditions, and also the higher stability of water–ethanol clusters. The existence of structures in which the alcohol molecules replace the water molecules was confirmed experimentally [14].

The low D values for phenol and guaiacol relative to those of ethanol are explained by their lower mobility due to the difference in the size of molecules. The average D values obtained here for phenol and guaiacol differ by 20%, but the error is also ~20%. The variation of the diffusion coefficients of phenol molecules reflects the existence of different structural units in solutions, which move at different rates. The formation of water–phenol clusters was proved experimentally in [15, 16], and the structure of aqueous, phenol, and water–phenol clusters was studied theoretically in [17]. It was shown that the stability of water–phenol clusters is close to that of water clusters, but the stability of phenol clusters is higher.

The diffusion coefficients of phenol in aqueous solutions at increased temperatures and pressures (of up to 673 K and 30 MPa) were experimentally determined by Taylor dispersion separation [18]. The authors noted a dramatic increase in the diffusion coefficient of phenol in water on passing to the SC region and near it. They performed modeling at a calculated density of fluid of 0.300 g/cm^3 (30.0 MPa, 673 K). Our data agree with the results of [18], taking into account the standard deviations in the self-diffusion coefficients (Table 2), though the mean values differ 1.5-fold. It should also be taken into account that in our study, the modeling was performed at a lower density, 0.133 g/cm^3, corresponding to the experimental pressure of 23.0 MPa.

In [19] the authors considered the solvation shell around phenol molecules in water under normal conditions. The spatial distribution functions were obtained for the oxygen and hydrogen atoms of water around the phenol molecule. They showed that under normal conditions, the water molecules form hydrogen bonds with the phenol OH group, and hydrogen bonds appear between the hydrogen atom of the water molecule and the π system of the benzene ring. The experimental data also suggest hydrogen bonding between the π system of the benzene ring of the phenol molecule as a proton acceptor and the water molecule as a proton donor [20]. The hydrogen bonds between the OH group of the phenol molecule and the water molecules below 363 K were theoretically studied in [21], which showed that phenol generally acts as a proton donor. According to the calculated data, the hydrogen bonds vanish near the critical point. In our study, it was obtained that at 673 K the diffusion coefficients of water were three times higher than for phenol; therefore, we can also draw the conclusion that the hydration shells of phenols are unstable under SC conditions.

While the solute molecules exist mainly as monomer units at a concentration of 2%, our data suggest their clusterization (Figs. 2 and 3). The higher stability of phenol clusters compared with water ones is indicated by the data of the theoretical work [17], which studied the structure and stability of phenol, water, and water–phenol clusters by the density functional method. The calculation showed that the intermolecular interaction in the phenol clusters is much stronger than that in the water clusters. The stability of the water–phenol clusters is close to that of the water clusters.

The authors of [18, 19, 21] calculated the model system consisting of one phenol molecule and 503 water molecules. This model system was inadequate for obtaining data on clusterization from solute molecules. Our calculated systems of 10000 molecules allowed us to obtain these data. The number of molecules in a cluster averaged over the whole calculation time for ethanol and phenol is 1.40 under normal conditions and 1.03 under supercritical conditions. At some steps of the trajectory, however, the cluster size was six or seven molecules for ethanol and five or six molecules for phenol under normal conditions, with dimers existing in the SC region, though single molecules were dominant. Clusterization was most pronounced for guaiacol: the number of single molecules decreased and the cluster size increased with time under normal conditions (colored insert, Fig. 4). For guaiacol under normal conditions, a cluster of two molecules was found, whose lifetime was 3 ns (colored insert, Fig. 5). In phenol and ethanol solutions, the tendency toward the enlargement of clusters with time is not pronounced. Clusterization of model lignin monomers in dilute solutions was also described. In particular, in aqueous solutions of tetrahydrofuran (THF), which is regarded as a monomer unit of lignin or the simple product of its chemical transformation, a molecular light scattering study revealed "nanodrops" with high THF contents [21]. As mentioned above, the calculation reported in [17] showed that phenol clusters are more stable than aqueous ones, which favors clusterization of phenol molecules under conditions of aqueous environment even at strong dilution. Clusterization of phenol molecules can explain the experimental predominant formation of the products of their condensation and pyrolysis on passing to SC conditions [4]. Several studies (e.g., [23]) showed that there is a concentration limit of phenol conversion into gaseous products (H_2, CO, CO_2, CH_4, C_2H_6): starting at a certain concentration, the

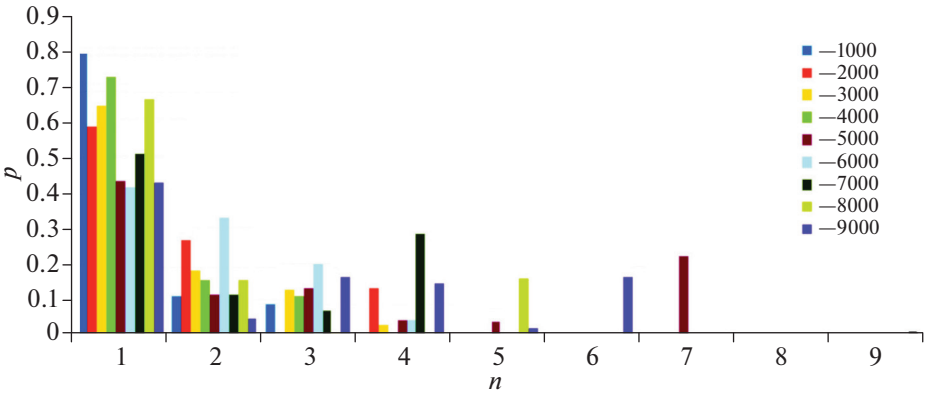

Fig. 4. Size distribution of agglomerates of guaiacol molecules at different trajectory steps for normal conditions: n is the number of molecules in the agglomerate, and p is the probability of existence of the agglomerate.

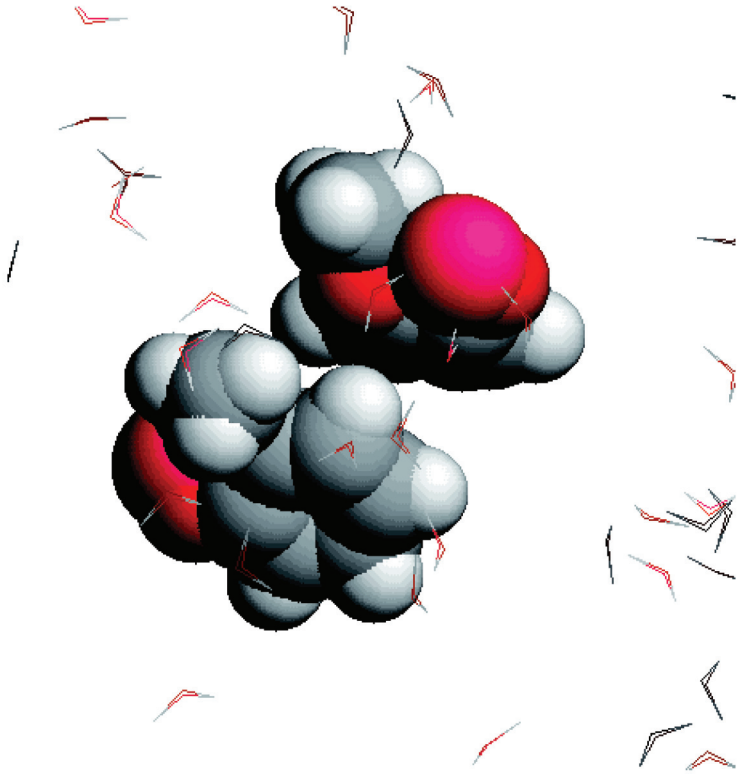

Fig. 5. Agglomerate of two guaiacol molecules surrounded by water molecules under supercritical conditions.

yield of phenol does not increase; in some cases, it even decreases, and condensation products start to form. Accordingly, for effective gasification, the process should be conducted in the range of concentrations at which phenols exist mainly as monomers.

CONCLUSIONS

A classical molecular dynamic modeling was performed of the structure of aqueous solutions containing 2 wt % ethanol, phenol, and guaiacol in NVT ensemble at densities of 0.997 g/cm^3 and 0.133 g/cm^3 corresponding to the normal (298 K, 0.1 MPa) and supercritical (673 K, 23.0 MPa) conditions, respectively. The radial distribution functions were calculated for the distances between the oxygen atoms of water molecules, the hydroxyl groups of solute molecules, and the centers of mass of phenol and guaiacol molecules. The self-diffusion coefficients were determined, and agglomeration of ethanol and phenol mol-

ecules under normal and supercritical conditions was analyzed. The results indicate that the solutions have an inhomogeneous composition. The solute molecules exist both as monomers and clusters. Clusters of up to seven molecules were found to form under normal conditions, and dimers were found under supercritical conditions. For guaiacol, clusterization is more pronounced than for ethanol and phenol. The structural features found for ethanol and phenol solutions under SC conditions were compared with each other, with the data for pure water, and with the experimental data on phenol transformations in supercritical water.

ACKNOWLEDGMENTS

This study was financially supported by the Russian Foundation for Basic Research (grant no. 18-29-06072).

REFERENCES

1. A. Corma, S. Iborra, and A. Velty, Chem. Rev. **107**, 2411 (2007).
2. H. Lasa, E. Salaices, J. Mazumder, and R. Lucky, Chem. Rev. **111**, 5404 (2011).
3. X. Wang, J. Zhou, H. Li, and G. Sun, Adv. Mater. Res. **821–822,** 1126 (2013).
4. V. I. Bogdan, A. V. Kondratyuk, A. E. Koklin, and V. V. Lunin, Russ. J. Phys. Chem. B **11**, 1207 (2017).
5. A. V. Kondratyuk, A. L. Kustov, V. V. Lunin, A. E. Koklin, and V. I. Bogdan, in *Proceedings of the 8th Conference with International Participation on Supercritical Fluids: Fundamentals, Technologies, Innovations, Zelenogradsk, Russia, Sept 14–19, 2015* (Kaliningrad, 2015), p. 219.
6. O. N. Fedyaeva and A. A. Vostrikov, Russ. J. Phys. Chem. B **6**, 844 (2012).
7. M. J. Abraham, D. Spoel, E. Lindahl, and B. Hess (GROMACS Development Team), *GROMACS User Manual, Version 5.0.7* (2015).
8. W. L. Jorgensen, D. S. Maxwell, and J. Tirado-Rives, J. Am. Chem. Soc. **118**, 11225 (1996).
9. W. L. Jorgensen, J. Chandrasekhar, J. D. Madura, et al., J. Chem. Phys. **79**, 926 (1983).
10. Thermophysical Properties of Fluid Systems. http://webbook.nist.gov.chemistry.fluid.
11. M. Smiechowski, C. Schran, H. Forbert, and D. Marx, Phys. Rev. Lett. **116**, 027801 (2016).
12. Yu. E. Gorbatyi and G. V. Bondarenko, Sverkhkt. Flyuidy: Teor. Prakt. **2** (2), 5 (2007).
13. P. M. Zorkii, L. V. Lanshina, and T. V. Bogdan, J. Struct. Chem. **49**, 524 (2008).
14. A. Wakisaka and K. Matsuura, J. Mol. Liq. **129**, 25 (2006).
15. K. Mizuse, T. Hamashima, and A. Fujii, J. Phys. Chem. A **113**, 12134 (2009).
16. T. Hamashima, K. Mizuse, and A. Fujii, J. Phys. Chem. A **115**, 620 (2011).
17. R. Parthasarathi, V. Subramanian, and N. Sathyamurthy, J. Phys. Chem. A **109**, 843 (2005).
18. A. Plugatyr and I. M. Svishchev, J. Phys. Chem. B **115**, 2555 (2011).
19. A. Plugatyr and I. M. Svishchev, J. Chem. Phys. **124**, 024507 (2006).
20. K. P. Gierszal, J. Davis, et al., Chem. Phys. Lett. **2**, 2930 (2011).
21. N. Zhang, X. Ruan, Y. Song, Z. Li, and G. He, J. Mol. Liq. **221**, 942 (2016).
22. N. F. Bunkin, A. V. Shkirin, G. A. Lyakhov, et al., J. Chem. Phys. **145**, 184501 (2016).
23. P. Changsuwana, N. Paksunga, Sh. Inoue, T. Inouel, Yo Rfwai, T. Noguchi, H. Tanigawa, and Yu. Matsumura, J. Supercrit. Fluids **142**, 32 (2018).

Translated by L. Smolina

SPELL: 1. OK